Shear Behavior of I-shaped Wood-steel Composite Beams

Shixu Wu,[a] Qifeng Shan,[a] Jialiang Zhang,[a] Keting Tong,[a] and Yushun Li [b,*]

To expand the application of wood as a building material, a new type of I-shaped wood-steel beam that consisted of laminated veneer lumber and cold-formed thin-walled steel was considered in this paper. The shear performance of nine wood-steel composite beams was tested to evaluate the effects of shear span ratio, web thickness, and flange thickness. Then, the failure pattern and failure mechanism of the composite beams were analyzed. The main affecting factors of shear capacities were also discussed. Furthermore, the calculation formula for bearing capacities of composite beams was established and the calculation results were compared with the experimental results. The experimental results showed that the combined effect of composite beams was excellent. The shear capacity was mainly affected by shear span ratio and web thickness. The calculation formula of the shear capacity was established based on the shear flow theory and the specification for structural steel buildings. The formula was derived from the micro-segment balance method and the reciprocal theorem of shear stress. The calculation results according to the formula were in good agreement with the experimental values.

Keywords: Composite beam; Laminated veneer lumber; Thin-walled steel; Shear span ratio; Shear capacity

*Contact information: a: School of Civil and Environmental Engineering, Ningbo University, Ningbo 315211, China; b: College of Civil Engineering & Architecture, Qingdao Agricultural University, Qingdao, 266109, China; *Corresponding author: lys0451@163.com*

INTRODUCTION

With the development of the construction industry, sustainable concepts, such as green and energy saving, are continuously promoted. It has become a trend to build efficient and environment-friendly structures in the construction industry today (Lou and Ren 2015). Wood is one of the most sustainable building materials. It has the advantages of low energy consumption, non-pollution, high strength ratio, and so on. Laminated veneer lumber (LVL) is a type of wooden plywood. The production method of unidirectional billet of LVL makes it more uniform and stable than solid timber, but it also has a few drawbacks, such as a small elastic modulus. Further, the mechanical properties of LVL are anisotropic and greatly affected by creep deformation. The strength in the perpendicular to grain direction of wood is noticeably different from the strength in the parallel-to-grain direction (Su 1990; Liu *et al*. 2007; Zhong *et al*. 2014). Therefore, it is of great significance for the development of the green construction industry to study wood composite members.

Steel has the advantages of high strength and homogeneous material. However, slender members cannot reach their ultimate strength because of local buckling or overall instability (Hou 2006). Through combining wood and steel in a reasonable way, the new type of composite structure can be formed to achieve the advantages of the two materials

fully (Bai and Jiang 2016). For example, the lateral rigidity of the wood is sufficient to prevent steel from premature buckling in the composite beam structure, and the steel can also strengthen the wood. The cooperation of the two materials could effectively improve the mechanical properties of the composite members.

Current studies on the mechanical properties of composite structures have been mainly focused on concrete-steel composite structures. As the concept of composite structures has been gradually recognized, some new types of composite structures have emerged and attracted great attention at home and abroad. Gutkowski *et al*. (2004) introduced a new type of composite structure. They used a solid wood layer instead of the cracked concrete and rebar of a solid concrete slab. The concrete slab thickness was reduced approximately 50%. The resulting composite structure exhibited excellent performance. Schanack *et al*. (2015) used small gaps to simulate the concrete cracking. Then, the authors further studied the mechanical properties of wood-concrete composite beams, which were affected by concrete cracking. The experiment showed that the slip modulus can decrease more than 70%. Kortiš *et al*. (2015) used finite element software (ADNIA) to analyze the junction performance of wood-steel composite beams and provided an effective method to simulate the composite beams with complex shapes. Jasieńko and Nowak (2014) studied wood-steel composite beams, which were formed by placing steel plates inside or outside of the wooden beams. The results showed that the mechanical performance of composite beams was excellent. Chen *et al*. (2016) proposed a welded H-shaped steel composite beam as the skeleton and pasted wooden boards on the outer surface of the steel beam to form an I-shaped section. Based on the test, the calculation method of mid-span deflection and bearing capacity was proposed. The research group of Ningbo University already studied the bending and shear properties of bamboo-steel composite structures (Li *et al*. 2011; Zhai *et al*. 2015). However, there have been few studies on the shear properties of wood-steel composite beams. Therefore, it is of great theoretical significance and engineering application value to conduct experimental research on the shear properties of wood-steel composite beams.

In this study, a new type of I-shaped wood-steel composite beam, which consisted of laminated veneer lumber and cold-formed thin-walled steel, is proposed. Nine composite beams proposed were tested in terms of shear span ratio, web thickness, and flange thickness. The shear failure mode and failure mechanism of composite beams were analyzed and compared. A formula for calculating the shear bearing capacities of composite beams is proposed based on the test results.

EXPERIMENTAL

Materials

The I-shaped composite beam was prepared with cold-formed thin-walled steel (Ningbo Haishu Shiqi Zhenren Material Management Department, Ningbo, China), LVL plywood (Guannan Yindelong Wood Industry Co., Ltd., Lianyungang, China), and structure adhesive (Henkel Adhesive Technology (Guangdong) Co., Ltd., Dongguan, China). The mechanical properties of materials including LVL plywood and the thin-walled steel of composite beams were tested in a structural laboratory. The thickness, yield strength, tensile strength, elastic modulus, Poisson ratio, and yield ratio of steel sheets were measured according to ISO 6892-1 (2016). The mechanical properties of steel are shown in Table 1.

The mechanical properties of LVL plywood used in this research were measured according to GB/T 17657 (2013). The shear strength of LVL plywood was 6.57 MPa, the elastic modulus was 13,373 MPa and the tensile strength was 85.28 MPa.

Table 1. Mechanical Properties of Steel

Thickness (mm)	Yield Strength (MPa)	Tensile Strength (MPa)	Elastic Modulus (MPa)	Poisson Ratio	Yield Ratio
1.5	256	350	2.15×10^5	0.26	0.81

Test Specimens

The composite beam was composed of two pieces of cold-formed thin-walled steel channel placed opposite each other as a skeleton and three pieces of LVL plywood. The specific production processes employed were as follows. First, the stains and galvanized layers were removed from the surface of the steel and plywood. Then, the polished steel and LVL plywood were wiped with alcohol to ensure that the bonding surfaces were clean. Finally, the steel channel and LVL plywood were combined with adhesive. The consumption of structural adhesive was determined according to the size of specimen, and pressure curing at 25 °C. The production process of composite beam is shown in Fig. 1.

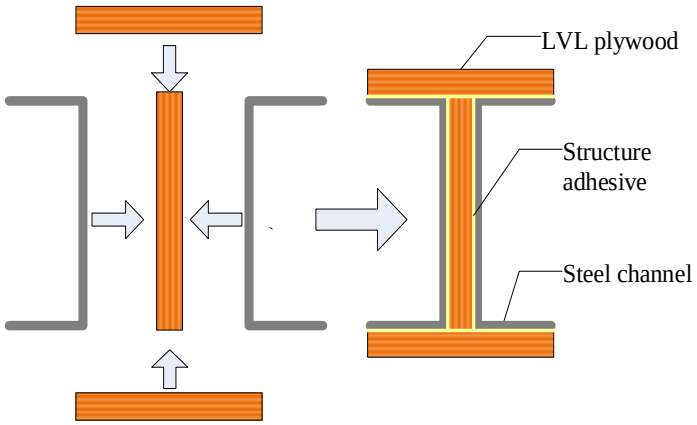

Fig. 1. Production process of composite beam

Fig. 2. LVL-steel composite beams

This combined method is convenient for processing and industrial production. The stability and buckling resistance of the composite beam has improved noticeably due to the restraining action of the LVL plywood. Nine I-shaped composite beams designed for the test are shown in Fig. 2 and numbered as L-1 to L-9 in order.

The main parameters of test specimens consisted of shear span ratio, web thickness, and flange thickness. The web thickness of test specimens included 20 mm and 25 mm, and the shear span ratio were 1.0, 1.5, 2.0, 2.5, and 3.0. The thickness of steel was 1.5 mm. The cross-section dimensions of steel channel (flange width × web height) were 30 mm × 120 mm. Nine test specimens, designated L-1 through L-9, were all designed as 1.80 m long, and the calculation span of specimens was 1.50 m. The parameters of specimens are shown in Table 2.

Table 2. Parameters of Specimens

Specimens	Web Thickness (mm)	Flange Thickness (mm)	Beam Section Size (mm)	Shear Span Ratio
L-1	20	20	80 × 160	1.0
L-2	20	25	80 × 170	1.0
L-3	20	20	80 × 160	1.5
L-4	25	20	85 × 160	1.5
L-5	25	25	85 × 170	2.0
L-6	25	20	85 × 160	2.0
L-7	20	20	80 × 160	2.5
L-8	25	20	85 × 160	2.5
L-9	25	20	85 × 160	3.0

Methods

The hydraulic pressure testing machine (Changchun New Testing Machine Co., Ltd., Changchun, China) was used as the reaction frame loading system in this study, and the distributive beam was used for two-point symmetrical loading, as shown in Fig. 3a.

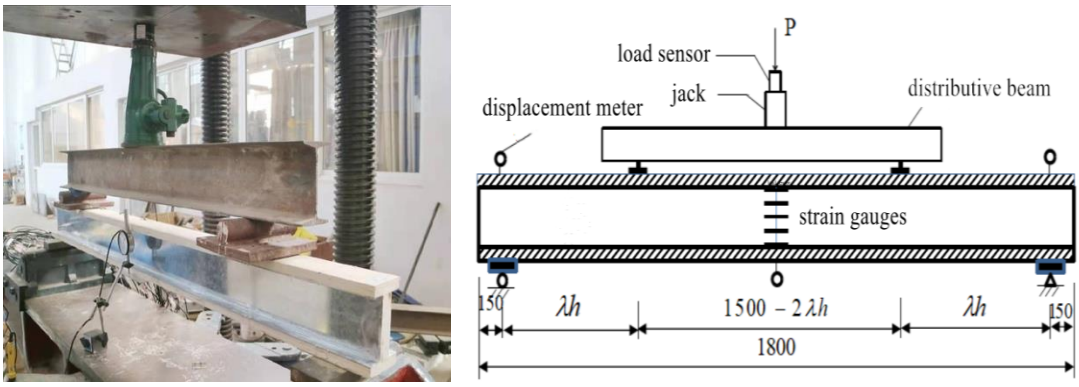

Fig. 3. (a) Test loading device and (b) schematic diagram of loading device (λ is the shear span ratio, h is the beam height, and all dimensions are in mm)

The method of monotonous multistage loading was adopted for the test. The load increment of each level was 4 kN. According to the requirements of grading loading, 10%

of the ultimate load was used as the increment of each level. The force sensor was adopted to measure the compressive load. Five strain gauges were evenly arranged at the web of the beams' mid-span. Displacement meters were arranged at the support point and mid-span of the specimens to record the change in deflection of the composite beams. A schematic of the loading device of the test is shown in Fig. 3b.

RESULTS AND DISCUSSION

Failure Mechanism and Test Observations

The mechanical properties of the composite beams were excellent during the loading test. The loading process can be divided into three stages: linear elastic stage, elastic-plastic stage, and failure stage. At the beginning of the test, the composite beams were in the stage of linear elasticity. Then, in the middle and later stages of the test, the classifications of composite beams can be made based on the failure mode.

The failure characteristics of the specimens (L-1 to L-4) were analogous, because the shear span ratio of the composite beams was similar. Taking L-3 as an example, subtle compressive cracks appeared at the support point when the load was up to 48 kN, and the deflection at the mid-span of the specimen was 4.07 mm at the same time. Then, as the applied load further increased, cracking and squeezing sounds appeared in the LVL plywood. The cracks at the support point spread along the interlayer until the load increased to 72 kN, and the deflection at the mid-span reached 6.29 mm. When the load increased to 96 kN, the mid-span deflection of the composite beam reached 9.65 mm. The steel channel of the lower flange at the beam end bent. The LVL plywood was damaged in the compression zones (Fig. 4).

(a) (b)

Fig. 4. Failure modes of L-3: (a) steel channel bent and (b) the lower flange plywood cracked

The shear span ratio of the specimens (L-5 and L-6) was 2.0. There was no difference between the two specimens except for the thickness of the flange, and their failure modes were similar. Taking L-6 as an example, when the load increased to 58 kN, a slight sound came from LVL plywood due to the squeezed fiber. The LVL plywood at the lower beam end cracked longitudinally. Meanwhile, the mid-span deflection was 6.72 mm. When the load increased to 81 kN, the thin-walled steel of upper flange at the loading point bent and the cracks appeared in the LVL plywood, which deepened gradually until the LVL plywood became damaged (Fig. 5).

Fig. 5. Failure modes of L-6: (a) the LVL plywood at the lower beam end cracked and (b) the LVL plywood cracked at the loading point

The composite beams (L-7 to L-9) were simultaneously subjected to bending and shearing because of the larger shear span ratio. Taking L-7 as an example, when the load increased to 57 kN, the cracks appeared on the edge of the LVL plywood at the lower flange of the composite beam. Meanwhile, the buckling of thin-walled steel channel appeared on the web of the specimen. The mid-span deflection reached 10.09 mm at the same time. When the load reached 70 kN, the composite beam became damaged due to the web of the specimen sheared at the loading point (Fig. 6).

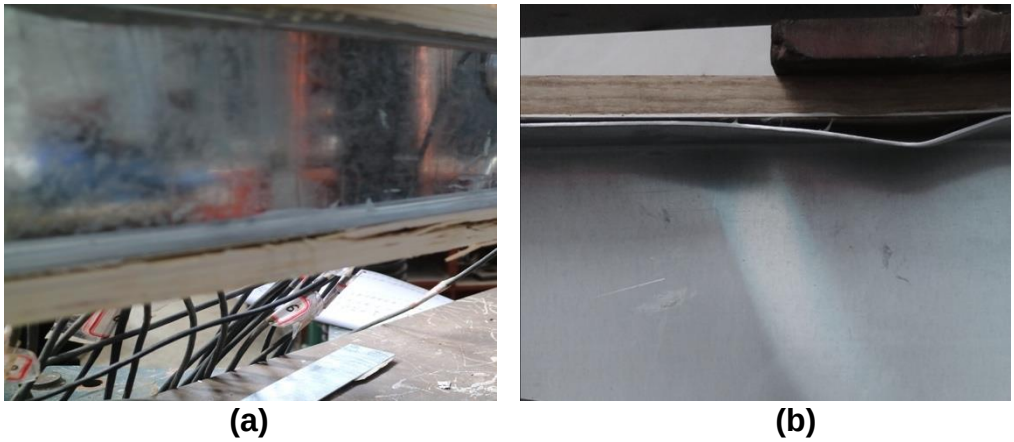

Fig. 6. Failure modes of L-7: (a) the lower flange plywood cracked at mid-span section and (b) the shearing failure of web at the loading point

Some conclusions could be drawn based on the phenomena described above, and the failure modes of the composite beams could be divided into three categories. The first conclusion was that when the shear span ratio was less than 2.0, the steel channel of the lower flange at the beam end bent, and the LVL plywood at the support point became cracked and damaged. The second was that when the shear span ratio was 2.0, the steel channel bent at the loading point, and the LVL plywood became cracked and damaged. The last one was that when the shear span ratio was greater than 2.0, the web of the composite beam became sheared and damaged at the loading point. When the shear span ratio changed from small to large, the failure modes of composite beams would be changed.

Load-deflection Curves

The load-deflection of mid-span curves of the composite beams in this test are shown in Fig. 7. It can be seen from the figure that the load-deflection curves of the specimens (L-1 to L-6) with the applied load increasing showed two stages. There were an elastic stage and an elastic-plastic stage. During the elastic stage, the load was less than 1/2 to 2/3 of the ultimate load. As the load increased, its deformation increased linearly. At this stage, LVL plywood and thin-walled steel worked together, and the overall performance of the composite beam was perfect. When the curves went into the elastic-plastic stages, the deformation developed quickly with increasing the applied load. At this time, the load had exceeded 1/2 to 2/3 of the ultimate load, and the load-deflection curves showed non-linear behavior. The mid-span deflection of the test specimens (L-7 to L-9) increased linearly with the increase of the load because of the relatively large shear span ratio. Eventually, the web at the loading point became sheared and destroyed, and the specimen reached its ultimate bearing capacity.

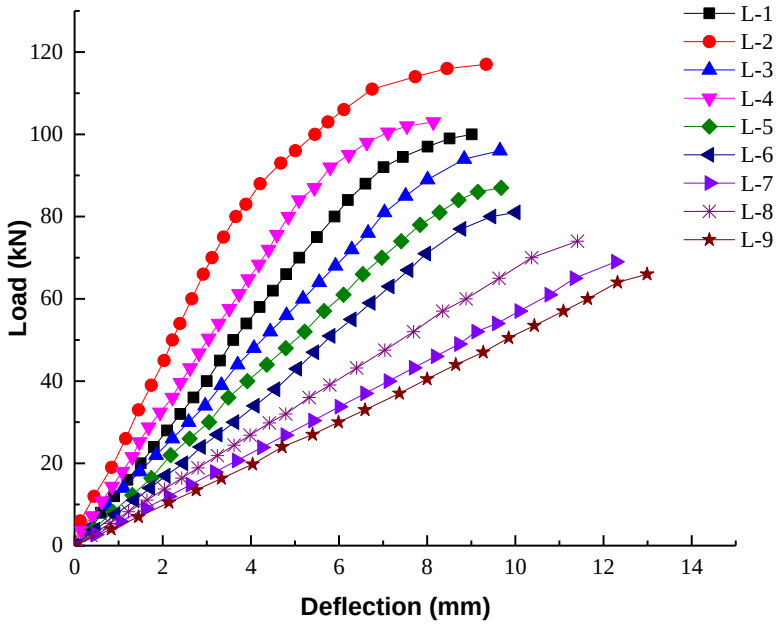

Fig. 7. Load-deflection of mid-span curves

Strains Distribution at Mid-span Section

Taking L-3 as an example, the cross-sectional strain curves of the specimen are shown in Fig. 8. Based on the analysis of the change of the strain at the neutral axis of the beam with the load, the strain at the neutral axis was always zero. As the load increased, the strain increased in the positive direction, and the strain distribution along the height at mid-span changed almost linearly. When the load reached 1/2 to 2/3 of the ultimate load, the position of neutral axis of section was at the center of the beam height. The plane remained after the bending deformation, which indicated that the deformation of the mid-span section of the composite beam accorded with the plane-section assumption.

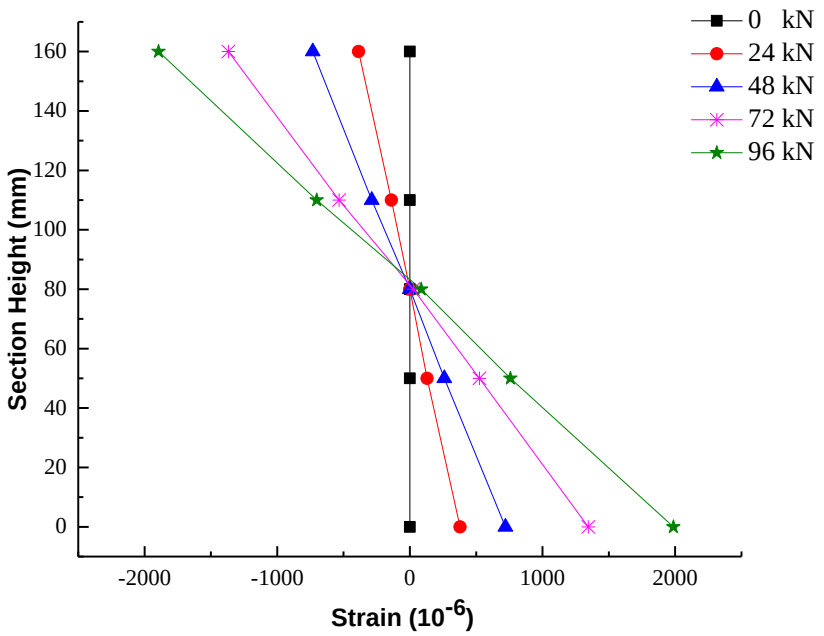

Fig. 8. Strain distribution at mid-span section of L-3

Bearing Capacity

According to GB 50017 (2017), $f \leq L/250$ was used as the control value of the mid-span deflection of the composite beam in the limit state of normal use. When the mid-span deflection of the composite beam reached 6 mm, it was considered to be the allowable deflection in the limit state of normal use. At this moment, the bending moment and shearing force of the test specimen were the section bearing capacity in the limit state of normal use. The main test results are shown in Table 3.

Table 3. Test Results

Specimens	Limit State of Normal Use		Limit State of Bearing Capacity		
	Shearing Force (kN)	Bending Moment (kN·m)	Shearing Force (kN)	Bending Moment (kN·m)	Mid-Span Deflection (mm)
L-1	42.0	6.72	50	8.48	9.01
L-2	52.5	8.93	58.5	9.95	9.34
L-3	34.0	8.16	48	11.52	9.65
L-4	46.5	11.16	51	12.96	8.14
L-5	30.0	10.20	43	15.81	9.68
L-6	26.0	8.32	40.5	13.12	10.01
L-7	16.5	6.60	35	13.60	12.28
L-8	20.0	8.00	37	15.00	11.41
L-9	15.0	7.20	34	15.36	12.99

PARAMETRIC ANALYSIS

For the specimens, the shear bearing capacities and failure modes are related to the shear span ratio, web thickness, and flange thickness.

Effect of Shear Span Ratio

The variations of the shear span ratio reflected the relationship between bending of beams and shear stress. As the shear span ratio increased, the failure modes and bearing capacities of the composite beams gradually changed. Taking specimens L-4, L-6, L-8, and L-9 as examples, the shear span ratio of L-9 was increased from 1.5 (shear span ratio of L-4) to 3.0, yet the ultimate load was reduced from 102 kN to 68 kN. The ultimate bearing capacity was reduced by 33.3%. Moreover, the deflection of the composite beam was increased from 8.14 mm to 12.99 mm. It can be seen that the shear capacity was negatively related to the shear span ratio. The shear span ratio actually reflected the relative relationship between normal stress and shear stress on the section. As the shear span ratio increased, the concentrated load was closer to the mid-span section, and its shear capacity would decrease. The load-deflection curves of the specimens are shown in Fig. 9.

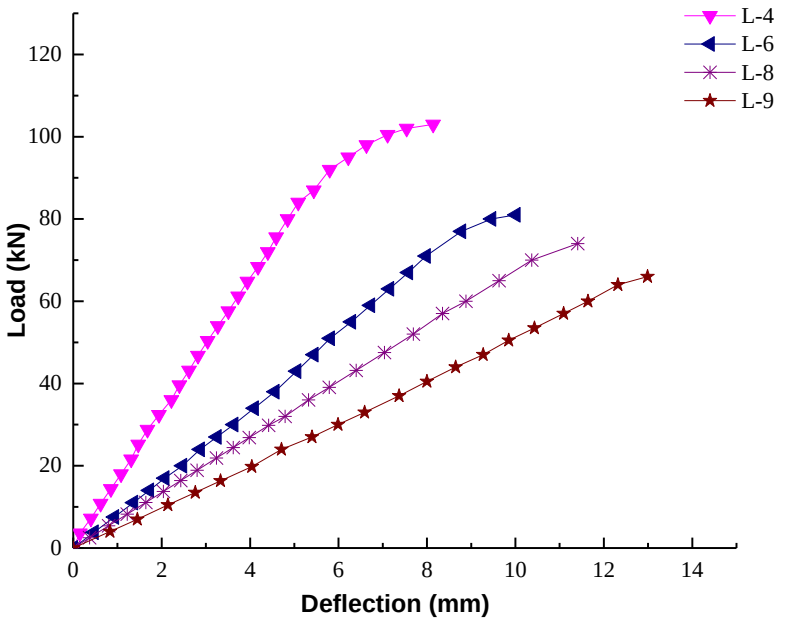

Fig. 9. Effect of shear span ratio on load-deflection curves

Effect of Web Thickness

Taking L-3, L-4, L-7, and L-8 as examples, the increase of web thickness could improve the ultimate bearing capacity of the composite beams. Through comparing load-deflection curves of specimens L-3 and L-4, the web thickness increased 5 mm, and the shear capacity increased 6.25%. For L-7 and L-8, the web thickness was also increased 5 mm, and the ultimate bearing capacity was increased 5.71%. The moment of inertia of the web section increased with the increase of the web thickness. Thus, the ultimate bearing capacity can be improved by increasing the web thickness of composite beams (Fig. 10).

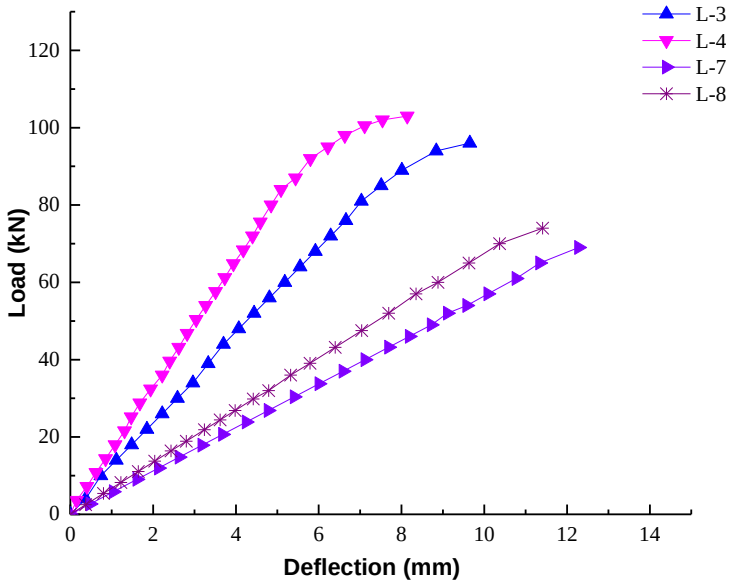

Fig. 10. Effect of web thickness on load-deflection curves

Effect of Flange Thickness

Taking specimens L-1, L-2, L-5, and L-6 as examples, it can be seen from the load-deflection curves of L-1 and L-2 that the flange thickness increased 5 mm, and the shear capacity increased 17%. For L-5 and L-6, the flange thickness increased 5 mm, and the ultimate bearing capacity increased 6.17%. The increase of the flange thickness can be essentially considered as an extension of the web of composite beams. The ultimate bearing capacity also increased (Fig. 11).

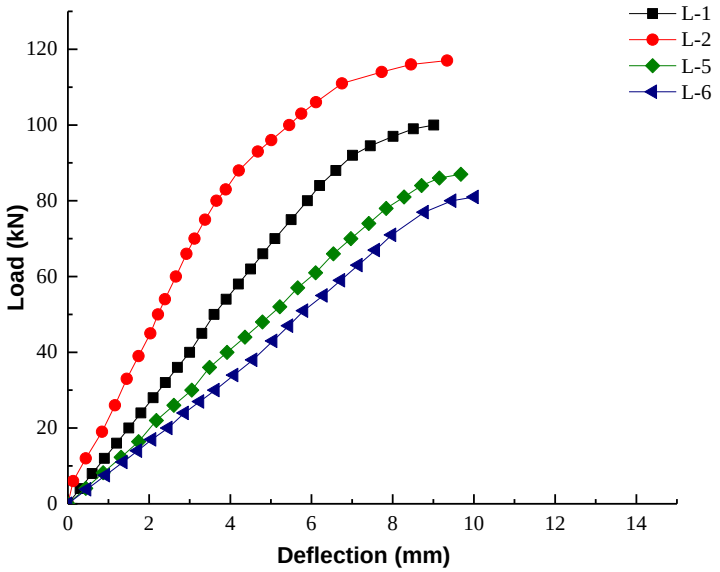

Fig. 11. Effect of flange thickness on load-deflection curves

THEORETICAL ANALYSIS AND VERIFICATION

Calculation Method of Shear Capacity

The test results were analyzed in this paper based on the literature (Lee and Yoo 1999; Nie *et al*. 2002; Xue *et al*. 2008; Xie 2012; Ge *et al*. 2018). When the bearing capacity of composite beams reached the ultimate load, the shear bearing capacity mainly consisted of the LVL plywood and steel. Thus, the superimposed calculation method was used in this paper,

$$V = V_{\mathrm{w}} + V_{\mathrm{s}} \tag{1}$$

where V is the shear capacity (kN) of the composite beam, V_{w} is the shear capacity (kN) of plywood of the composite beam, and V_{S} is the shear capacity (kN) of steel of the composite beam.

The calculation formula of plywood was established mainly based on the bending shear flow theory of thin-walled beams in material mechanics. The shear stress of the I-beam web only acted in the vertical direction. The maximum shear stress occurred at the neutral axis while the smallest stress occurred at the junction of the web and the flange. This stress was much greater than the shear stress of the flange. According to the literature (Triantafillou 1998; Tang 2014), the contribution coefficient (ζ = 1.04) of the flange was proposed in this paper due to the influence of shearing capacity of flange plywood.

The bonding strength between the parts of composite beam must be sufficient to transfer the shear stress. Assume that the shear stress at the neutral axis uniformly distributed across the web. Using the micro-segment balance method and the reciprocal theorem of shear stress, the calculation formula of the shear capacity can be derived as,

$$V_{\mathrm{w}} = \frac{\zeta f_{\mathrm{v}} I_{\mathrm{n}} b}{S_{\mathrm{n}}} \tag{2}$$

where f_{v} is the shear strength (MPa) of the plywood, b is the web thickness (mm), I_{n} is the moment of inertia of the web section, $I_{\mathrm{n}} = bh^3 / 12$, S_{n} is static moment of web section, $S_{\mathrm{n}} = bh^2 / 8$.

The calculation formula of shear capacity of steel mainly referred to ANSI/AISC 360-10 (2010). Based on the I-shaped section of the beam, the calculation formula of the shear capacity of steel was established,

$$\begin{aligned} &h_{\mathrm{w}} / t_{\mathrm{ws}} \le 1.1\sqrt{k_{\mathrm{v}} E / f_{\mathrm{y}}} \\ &V_{\mathrm{s}} = 0.6 f_{\mathrm{y}} t_{\mathrm{ws}} h_{\mathrm{w}} / 1+\lambda \end{aligned} \tag{3}$$

$$\begin{aligned} &h_{\mathrm{w}} / t_{\mathrm{ws}} > 1.1\sqrt{k_{\mathrm{v}} E / f_{\mathrm{y}}} \\ &V_{\mathrm{s}} = \left(0.6 f_{\mathrm{y}} t_{\mathrm{ws}} h_{\mathrm{w}} / 1+\lambda\right)\left(C_{\mathrm{v}} + \frac{1-C_{\mathrm{v}}}{1.15\sqrt{1+\left(a/h_{\mathrm{w}}\right)^2}}\right) \end{aligned} \tag{4}$$

where f_{y} is the tensile strength (MPa) of the steel, h_{w} is the web height (mm) of the steel, t_{ws} is the thickness (mm) of the steel, E is the elastic modulus (MPa) of the steel, C_{v} is the ratio of the critical buckling stress and the buckling stress of the web plate, a is the clear distance (mm) between transverse stiffeners, and k_{v} is the web plate shear buckling coefficient, $k_{\mathrm{v}} = 5 + 5 / (a/h_{\mathrm{w}})^2$.

For webs without transverse stiffeners, the clear distance between the transverse stiffeners of the composite beam can be regarded as infinite. Thus, the web plate shear buckling coefficient in this paper takes $k_v = 5$,

$$1.10\sqrt{k_v E / f_y} \le h_w / t_{ws} \le 1.37\sqrt{k_v E / f_y}$$

$$C_v = \frac{1.10\sqrt{k_v E / f_y}}{h_w / t_{ws}} \quad (5)$$

$$h_w / t_{ws} > 1.37\sqrt{k_v E / f_y}$$

$$C_v = \frac{1.51 k_v E}{\left(h_w / t_{ws}\right)^2 f_y} \quad (6)$$

Analysis of Results

The theoretical calculation values of the shear capacity of the composite beams were compared with the experimental values, and the calculation results were in good agreement with the experimental ones in Table 4. The experimental errors were less than 10%.

Table 4. Comparison of Shear Capacities Between Theoretical and Experimental Values

Specimens	Shear Span Ratio	V (kN)	V' (kN)	V'_w (kN)	V'_s (kN)	Δ (%)
L-1	1.0	50	52.38	14.58	37.8	4.75%
L-2	1.0	58.5	53.29	15.49	37.8	8.91%
L-3	1.5	48	44.82	14.58	30.24	6.63%
L-4	1.5	51	48.46	18.22	30.24	4.98%
L-5	2.0	43	44.56	19.36	25.2	3.63%
L-6	2.0	40.5	43.42	18.22	25.2	7.21%
L-7	2.5	35	36.18	14.58	21.6	3.36%
L-8	2.5	37	39.82	18.22	21.6	7.62%
L-9	3.0	34	37.12	18.22	18.9	9.18%

V is the experimental value, V' is the theoretical calculation value, V'_w is theoretical value of the plywood, V'_s is the theoretical value of the steel, and Δ means error, $\Delta = \left|\frac{V'-V}{V}\right| \times 100\%$

CONCLUSIONS

1. The I-shaped wood-steel composite beams were found to have a good overall performance. The shear capacity of the composite beams can reach 1/2 of the ultimate bearing capacity in the limit state of normal use. The advantages of LVL plywood and thin-walled steel are fully utilized.
2. The shear bearing capacities and failure modes are related to the shear span ratio, web thickness, and flange thickness. The bearing capacity increases with the increase of the web thickness of the composite beams. However, the shear capacity is negatively

related to the shear span ratio. The increase of the flange thickness can be essentially considered as an extension of the web of composite beams, and that can also improve the bearing capacities of the composite beam.

3. When the composite beams are subjected to bending and shearing simultaneously, the ultimate shear capacity will be reduced due to the presence of bending forces. In the design stage, it is necessary to consider that the web must be stable enough to ensure that the steel will not bend before reaching the ultimate shear capacity.
4. The calculation formula of the shear capacity was established based on the shear flow theory and ANSI/AISC 360-10 (2010). It is derived from the micro-segment balance method and the reciprocal theorem of shear stress. The calculation results according to the formula are in good agreement with the experimental values, and the average error is 6.25%.

ACKNOWLEDGMENTS

The authors are grateful for the support of the National Natural Science Foundation of China (51678310, 51978345), Zhejiang Provincial Natural Science Foundation of China (LQ19E080007), and the Ningbo Science and Technology project (202002N3090).

REFERENCES CITED

ANSI/AISC 360-10 (2010). "Specification for structural steel buildings," American Institute of Steel Construction, Chicago, IL, USA.

Bai, R. S., and Jiang, Z. L. (2016). "Research on steel-wood composite structure," *Journal of Hebei Institute of Architectural Engineering* 34(3), 75-78. DOI: 10.3969/j.issn.1008-4185

Chen, A. G., Li, D. H., Fang, C., Zheng, Q. G., and Xing, J. H. (2016). "Experimental study on flexural behavior of H-shaped steel-wood composite beams," *Journal of Building Structures* 37(S1), 261-267. DOI: 10.14006/j.jzjgxb.2016.S1.037

GB/T 17657 (2013). "Test methods of evaluating the properties of wood-based panels and surface decorated wood-based panels," Standardization Administration of China, Beijing, China.

GB 50017 (2017). "Standard for design of steel structures," Standardization Administration of China, Beijing, China.

Ge, Y. M., Li, Y. S., Tong, K. T., and Zhang, J. L. (2018). "Study on shear behavior of thin-wall steel-recombinant bamboo composite beams," *Forest Engineering* 34(6), 72-79. DOI: 10.16270/j.cnki.slgc.2018.06.031

Gutkowski, R. M., Brown, K., Shigidi, A., and Natterer, J. (2004). "Investigation of notched composite wood–concrete connections," *J. Struct. Eng.* 130(10), 1553-1561. DOI: 10.1061/(ASCE)0733-9445(2004)130:10(1553)

Hou, J. F. (2006). *The Research of Modern Timber Architecture Compound with Steel*, Master's Thesis, Southeast University, Nanjing, Jiangsu Province, China.

ISO 6892-1 (2016). "Metallic materials—Tensile testing—Part 1: Method of test at room temperature," International Organization for Standardization, Geneva, Switzerland.

Jasieńko, J., and Nowak, T. P. (2014). "Solid timber beams strengthened with steel plates – Experimental studies," *Constr. Build. Mater.* 63, 81-88. DOI: 10.1016/j.conbuildmat.2014.04.020

Kortiš, J., Gocál, J., Bednár, M., and Bátorek, V. (2015). "Use of orthotropic plastic material for stress analysis of double-shear-plane timber-steel structural connection," *Procedia Eng.* 111, 431-435. DOI: 10.1016/j.proeng.2015.07.112

Lee, S. C., and Yoo, C. H. (1999). "Experimental study on ultimate shear strength of web panels," *J. Struct. Eng.* 125(8), 838-846. DOI: 10.1061/(ASCE)0733-9445(1999)125:8(838)

Liu, H. R., Liu, J. L., and Chai, Y. B. (2007). "Application and development of laminated veneer lumber," *China Wood-Based Panels* 14(2), 5-7. DOI: 10.3969/j.issn.1673-5064.2007.02.002

Li, Y. S., Shen, H. Y., Shan, W., Lv, B., and Jiang, T. Y. (2011). "Experimental study on shear behavior of I-shaped section bamboo-steel composite beams," *Journal of Building Structures* 32(7), 80-86. DOI: 10.14006/j.jzjgxb.2011.07.012

Lou, W. L., and Ren, H. Q. (2015). "Characteristics and prospects of wood structure buildings in China," *China Wood Industry* 29(5), 20-23. DOI: 10.3969/j.issn.1001-8654.2015.05.005

Nie, J. G., Chen, L., and Xiao, Y. (2002). "Composite shear behavior of steel-concrete composite beams under sagging moment," *Journal of Tsinghua University (Science and Technology)* 42(6), 835-838. DOI: 10.16511/j.cnki.qhdxxb.2002.06.034

Schanack, F., Ramos, O. R., Reyes, J. P., and Low, A. A. (2015). "Experimental study on the influence of concrete cracking on timber concrete composite beams," *Eng. Struct.* 84, 362-367. DOI: 10.1016/j.engstruct.2014.11.041

Su, F. M. (1990). "A new type of structural material laminated veneer lumber," *Jiangxi Forestry Science and Technology* 1990(1), 41-43. DOI: 10.16259/j.cnki.36-1342/s.1990.01.025

Tang, J. (2014). *Study on Mechanical Properties of Reconstituted Bamboo-steel Composite Beam*, Master's Thesis, Ningbo University, Zhejiang Province, China.

Triantafillou, T. C. (1998). "Composites: A new possibility for the shear strengthening of concrete, masonry and wood," *Compos. Sci. Technol.* 58(8), 1285-1295. DOI: 10.1016/S0266-3538(98)00017-7

Xie, Q. T. (2012). *Research on Bond Property of Steel-Bamboo Interface Under Static Loads*, Master's Thesis, Ningbo University, Ningbo, Zhejiang Province, China.

Xue, J. Y., Cheng, G., Zhao, H. T., and Fu, G. (2008). "Experimental study on shear behavior of steel-concrete composite beams under negative moment," *Journal of Building Structures* 2008(S1), 83-87. DOI: 10.14006/j.jzjgxb.2008.s1.022

Zhai, J. L., Li, Y. S., Huang, S., and Du, Y. F. (2015). "Experimental study on seismic behavior of steel-bamboo composite frame structure," *Journal of Building Structures* 36(S1), 60-66. DOI: 10.14006/j.jzjgxb.2015.S1.010

Zhong, Y., Xing, X. T., Ren, H. Q., and Zhang, R. (2014). "Properties of structural laminated veneer lumber in compression at an angle to grain," *Journal of Building Materials* 17(1), 115-119. DOI: 10.3969/j.issn.1007-9629.2014.01.021

Article submitted: September 21, 2020; Peer review completed: November 15, 2020; Revised version received: November 19, 2020; Accepted: November 20, 2020; Published: November 25, 2020.
DOI: 10.15376/biores.16.1.583-596